Available online at www.sciencedirect.com
ScienceDirect
Polymer 48 (2007) 5250–5258
polymer
www.elsevier.com/locate/polymer

Synthesis and characterization of amphiphilic graft copolymers with hydrophilic poly(acrylic acid) backbone and hydrophobic poly(methyl methacrylate) side chains

Dan Peng, Xiaohuan Zhang, Chun Feng, Guolin Lu, Sen Zhang, Xiaoyu Huang*

Laboratory of Polymer Materials and Key Laboratory of Organofluorine Chemistry, Shanghai Institute of Organic Chemistry, Chinese Academy of Sciences, 354 Fenglin Road, Shanghai 200032, PR China

Received 29 January 2007; received in revised form 23 May 2007; accepted 2 July 2007
Available online 27 July 2007

Abstract

A series of well-defined amphiphilic graft copolymers containing hydrophilic poly(acrylic acid) backbones and hydrophobic poly(methyl methacrylate) side chains were synthesized by successive atom transfer radical polymerization followed by the selective hydrolysis of poly(methoxymethyl acrylate) backbone. Grafting-from strategy was employed for the synthesis of graft copolymers with narrow molecular weight distributions. Hydrophobic side chains were connected with the backbone through stable C–C bonds instead of ester connections. The backbone can be easily hydrolyzed to poly(acrylic acid) with HCl without affecting the hydrophobic side chains. The amphiphilic graft copolymers can form stable micelles in water. The critical micelle concentration was determined by fluorescence spectroscopy. The micellar morphologies were found to be vesicles by transmission electron microscopy and changed to spheres with the addition of NaCl.

Keywords: Graft copolymer; ATRP; Grafting-from

1. Introduction

The self-assembly behavior of amphiphilic copolymers in water has been extensively studied for decades [1–4]. Previous studies showed that experimental parameters, such as molecular weight, composition and architecture of the copolymer, solvent quality, concentration, and temperature, could affect the aggregation number, the size and the shape of the micelles [5–7]. So far, most of the investigations have been concerned with the micellization of linear block copolymers [2–4]. Graft copolymers may form a variety of micellar shapes due to their complicated and confined structure [8,9]. Due to the theoretical and experimental potential aspects, additional studies on amphiphilic graft copolymers are needed in order to elucidate the influence of the architecture and composition on the micellization.

The synthesis of well-defined graft copolymers is much more difficult compared with the synthesis of linear block copolymers, which restrained the studies of the self-assembly behavior of the more complex structured materials. Generally, three strategies, including grafting-through, grafting-onto and grafting-from, were used to synthesize the graft copolymers [10–14]. For the grafting-from strategy, the pendant initiation groups on the backbone can initiate the polymerization of the corresponding monomer to form side chains. Recently, well-defined graft copolymers with hydrophobic backbone and hydrophilic side chains were synthesized by the combination of atom transfer radical polymerization (ATRP) [15,16] and grafting-from techniques, and their self-assembly behaviors were preliminarily explored [10,17]. Unfortunately, there are only few reports about the synthesis of well-defined graft copolymers with hydrophilic backbone and hydrophobic side chains, as well as self-assembly behaviors in aqueous media [8,18–20].

This article describes the synthesis and characterization of amphiphilic graft copolymers with hydrophilic poly(acrylic

* Corresponding author. Tel.: +86 21 54925310; fax: +86 21 64166128.
E-mail address: xyhuang@mail.sioc.ac.cn (X. Huang).

0032-3861/$ - see front matter © 2007 Elsevier Ltd. All rights reserved.
doi:10.1016/j.polymer.2007.07.005

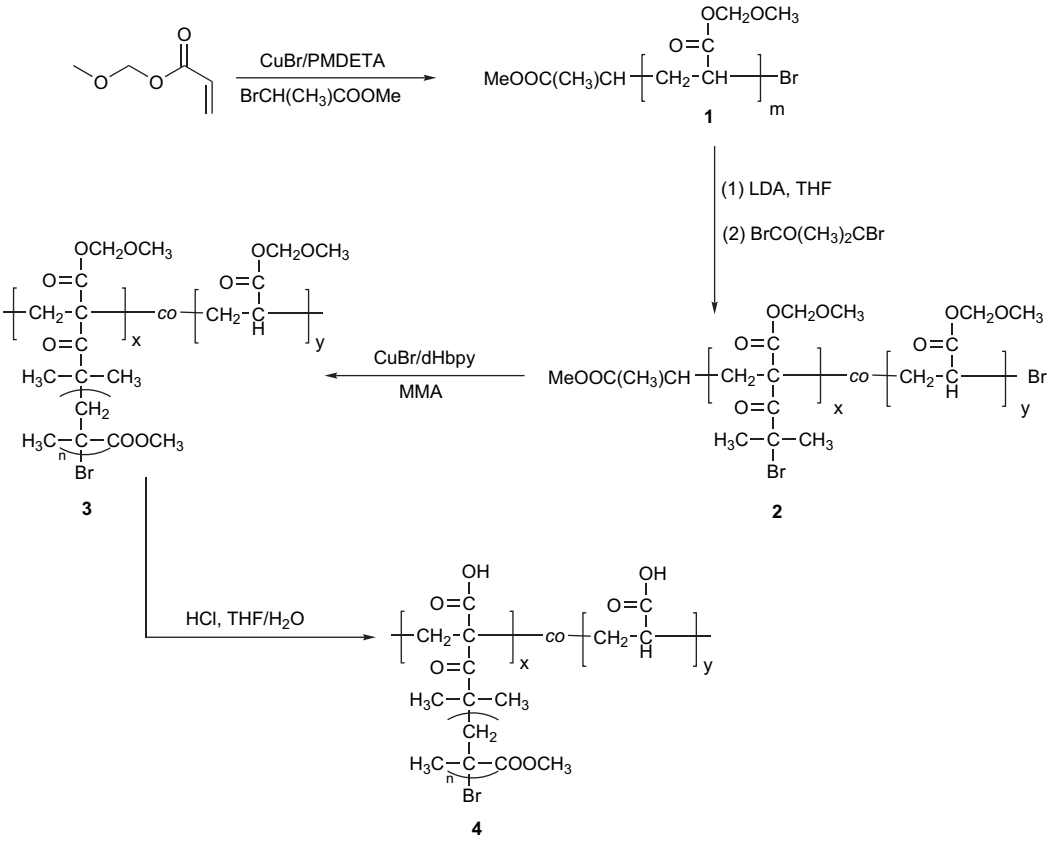

Scheme 1. Synthesis of PAA-*g*-PMMA amphiphilic graft copolymer.

acid) (PAA) backbone and hydrophobic poly(methyl methacrylate) (PMMA) side chains by ATRP and grafting-from techniques exhibiting narrow polydispersities (Scheme 1). This kind of amphiphilic graft copolymer can form vesicle micelles in aqueous media. The critical micelle concentration (cmc) of these graft copolymers in water was measured by fluorescence spectroscopy as well as the shapes and sizes of the micelles under different conditions were studied by transmission electron microscopy (TEM).

2. Experimental

2. 1. Materials

Methyl methacrylate (MMA, Aldrich, 99%) was washed with 5% aqueous NaOH solution to remove the inhibitor, then washed with water, dried over $CaCl_2$ and distilled twice over CaH_2 under reduced pressure just before use. Copper(I) bromide (CuBr, Aldrich, 98%) was purified by stirring overnight over CH_3CO_2H at room temperature, followed by washing the solid with ethanol, diethyl ether and acetone prior to drying at 40 °C under vacuum for 1 day. Diisopropylamine (Aldrich, 99.5%) was dried over KOH for several days followed by distilling from CaH_2 under N_2 atmosphere. Tetrahydrofuran (THF) was dried over CaH_2 for several days and distilled from sodium and benzophenone under N_2 atmosphere prior to use. *N*,*N*,*N*′,*N*′,*N*″-Pentamethyldiethylenetriamine (PMDETA, Aldrich, 99%), methyl 2-bromopropionate (2-MBP, Acros, 99%), *n*-butyllithium (*n*-BuLi, Aldrich, 1.6 M in hexane) and α-bromoisobutyryl bromide (TCI, 98%) were used as received. Methoxymethyl acrylate (MOMA) and 4,4′-diheptyl-2,2′-bipyridine (dHbpy) were synthesized according to the previous literatures [19,21].

2.2. Measurements

FT-IR spectra were recorded on a Nicolet AVATAR-360 FT-IR spectrophotometer with 4 cm^{-1} resolution. All ^1H NMR and ^{13}C NMR measurements were performed on a Varian Mercury 300 spectrometer (300 MHz) in $CDCl_3$. TMS (^1H NMR) and $CDCl_3$ (^{13}C NMR) were used as internal standards. Bromine content was determined by the titration with $Hg(NO_3)_2$. Conversion of MMA was determined by gas chromatography (GC) using a HP 6890 system with an SE-54 column. Relative molecular weights and molecular weight distributions were determined by gel permeation chromatography (GPC) system equipped with a Waters 1515 Isocratic HPLC pump, a Waters 2414 refractive index detector (RI), a Waters 2487 dual absorbance detector (UV, $\lambda =$ 260 nm) and a set of Waters Styragel columns (HR3, HR4 and HR5, 7.8 × 300 mm). GPC measurements were carried out at 35 °C using THF as eluent with a 1.0 mL/min flow rate. The system was calibrated with linear polystyrene standards. Steady-state fluorescent spectra were recorded on a Perkin Elmer LS55 spectrofluorometer with the bandwidth of 15 nm for excitation and 3 nm for emission, where λ_{ex}

was 339 nm. TEM images were obtained using a Philips CM120 instrument operated at 80 kV.

2.3. Polymerization of MOMA by ATRP

Poly(methoxymethyl acrylate) (PMOMA) **1** was prepared by ATRP of MOMA initiated by 2-MBP. A typical procedure is listed as follows: CuBr (0.2355 g, 1.65 mmol) was first added to a 25 mL Schlenk flask (flame-dried under vacuum prior to use), sealed with a rubber septum for degassing and kept under N_2 atmosphere. Next, MOMA (5.0 mL, 42.8 mmol) and PMDETA (0.34 mL, 1.65 mmol) were introduced via a gas-tight syringe and the mixture was stirred for several minutes. Finally, 2-MBP (0.18 mL, 1.65 mmol) was added via a gas-tight syringe. The solution was degassed by three cycles of freeze–pump–thaw followed by immersing the flask into an oil bath thermostated at 50 °C in order to start the polymerization. The polymerization was terminated by placing the flask into liquid nitrogen after 2.5 h. THF was added to dissolve the viscous crude product and the solution was filtered through a short Al_2O_3 column to remove the copper catalyst. The resulting solution was concentrated and precipitated in hexane. After repeated purification by dissolving in THF and precipitating in hexane for three times, 3.8859 g glassy solid (PMOMA **1a**) was obtained with a yield of 78%, $M_n = 3600$, $M_w/M_n = 1.14$. FT-IR (film): ν (cm^{-1}): 2957 (–C–H), 1740 (C=O), 1144, 1088 (C–O–C), 925. ^{1}H NMR ($CDCl_3$): δ (ppm): 1.09 (d, 3H, CH_3CH), 1.51, 1.68, 1.96 (br, 2H, CH_2CH), 2.34 (br, 1H, CH$_2$CH), 3.40 (s, 3H, OCH_3), 4.25 (t, 1H, CHBr), 5.16 (s, 2H, COOCH_2O). ^{13}C NMR ($CDCl_3$): δ (ppm): 33.3–36.9 (CH_2CH), 41.4 (CH$_2$CH), 57.8 (–OCH_3), 90.6 (COOCH_2O), 173.9 (COOCH$_2$). Br%: 2.21%.

2.4. Synthesis of PMOMA-Br macroinitiator **2**

Dried THF (20 mL) and diisopropylamine (2.8 mL, 20.0 mmol) were added to a 250 mL three-necked flask sealed with rubber septa. The solution was cooled to −78 °C and *n*-BuLi (1.6 M, 11.2 mL, 17.9 mmol) was added slowly. After 1 h, the mixture was treated with a 100 mL solution of PMOMA **1a** (1.7553 g, $M_n = 3600$, $M_w/M_n = 1.14$) and THF at −78 °C. The reaction lasted for 7 h. Next, α-bromoisobutyryl bromide (2.5 mL, 20.2 mmol) was introduced. After 4 h, the reaction was terminated by adding deionized water. The organic phase was washed with water and brine, and was left to dry over $MgSO_4$ overnight. After filtration, the filtrate was concentrated and precipitated in hexane. The product was dried under vacuum to give 1.2043 g of yellow powder (PMOMA-Br **2a**). $M_n = 3300$, $M_w/M_n = 1.27$. FT-IR (film): ν (cm^{-1}): 2957, 1740, 1252, 1212, 1159, 1092, 912. ^{1}H NMR ($CDCl_3$): δ (ppm): 1.0–3.3 (br, protons on PMOMA backbone), 1.97 (s, 6H, C(CH_3)$_2$Br), 3.50 (s, 3H, –OCH_3), 5.28 (s, 2H, COOCH_2O). ^{13}C NMR ($CDCl_3$): δ (ppm): 19.1, 21.2 (C(CH_3)$_2$Br), 24.3–36.5 (CH_2CH), 39.0, 41.1 (CH$_2$CH), 47.8 (*tert-C* on PMOMA backbone), 55.0 (C(CH$_3$)$_2$Br), 57.6 (OCH_3), 93.2 (COOCH_2O), 170.3, 174.0 (O–C=O), 207.4 (C–C=O). Br%: 8.83%.

2.5. Synthesis of graft copolymer PMOMA-g-PMMA **3**

In a typical procedure, CuBr (0.0146 g, 0.10 mmol) was charged to a dried 25 mL Schlenk flask. The flask was degassed and CuBr was kept under N_2 atmosphere. Next, dHbpy (0.0711 g, 0.20 mmol) and MMA (5.3 mL, 49.7 mmol) were introduced via a gas-tight syringe. Finally, PMOMA-Br **2a** (0.0809 g, $M_n = 3300$, $M_w/M_n = 1.27$, Br%: 8.83%) was added. The flask was degassed by three cycles of freeze–pump–thaw and followed by immersing into an oil bath thermostated at 50 °C. After 10 min, the polymerization was terminated by placing the flask into liquid N_2. The reaction mixture was diluted with THF and filtered through a short Al_2O_3 column to remove the copper catalyst. After concentration, PMOMA-*g*-PS **3b** was obtained by precipitation in methanol and dried under vacuum (0.1453 g, $M_n = 24{,}000$, $M_w/M_n = 1.25$). FT-IR (film): ν (cm^{-1}): 2996, 2951, 1731, 1272, 1243, 1193, 1150, 917. ^{1}H NMR ($CDCl_3$): δ (ppm): 0.78, 0.96, 1.18 (s, 3H, CH_3), 1.36, 1.53–2.10 (br, 2H, CH_2), 2.64 (br, 1H, CH on PMOMA backbone), 3.45 (s, 3H, CH$_2$OCH_3), 3.57 (s, 3H, COOCH_3), 5.21 (s, 2H, COOCH_2O).

2.6. Hydrolysis of PMOMA backbone

Graft copolymer, PMOMA-*g*-PMMA, was dissolved in THF and treated with an excess of 1 M HCl for 2 h at room temperature. The reaction mixture was washed with water until the aqueous phase became neutral (pH = 7). The solution was further washed with brine and dried over $MgSO_4$. After filtration, the filtrate was concentrated and precipitated in hexane. The final white solid was dried under vacuum. FT-IR (film): ν (cm^{-1}): 3457, 2990, 2950, 1731, 1272, 1242, 1192, 1149. ^{1}H NMR ($CDCl_3$): δ (ppm): 0.83, 1.01, 1.22, (s, 3H, CH_3), 1.40, 1.58–2.28 (br, 2H, CH_2), 2.71 (br, 1H, CH on PMOMA backbone), 3.59 (s, 3H, COOCH_3). For GPC analysis, poly(acrylic acid) backbone was reprotected to poly(methyl acrylate) backbone by CH_2N_2 as shown in the following scheme (Scheme 2).

2.7. Determination of critical micelle concentration

Pyrene was used as the fluorescence probe. The acetone solution of pyrene (60 mg/L, 2.97×10^{-4} mol/L) was added to water until the concentration of pyrene reached 5×10^{-7} mol/L. Next, different amounts of PAA-*g*-PMMA **4** (hydrolysis product of PMOMA-*g*-PMMA **3**) solutions in THF (1 mg/mL) were added to water containing pyrene ([pyrene] = 5×10^{-7} mol/L). All fluorescence spectra were recorded at 25 °C.

2.8. TEM images

To prepare micelles, PAA-*g*-PMMA **4** solution in THF (1 mg/mL) was added dropwise to water with vigorous stirring until the final concentration reached 0.05 mg/mL (the volume of THF was approximately 5% of the final solution). The solution was stirred for another several hours for the evaporation

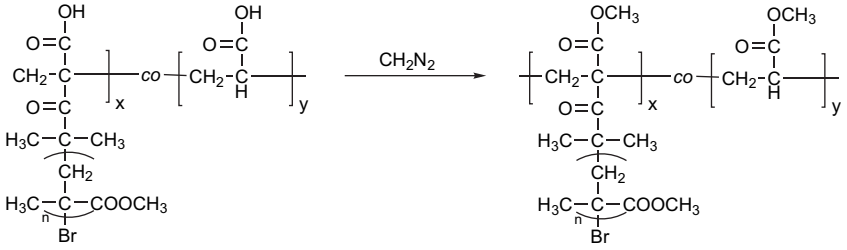

Scheme 2. Reprotection of poly(acrylic acid) backbone.

of THF. For TEM studies, 0.01 mL of micellar solution was deposited on an electron microscopy copper grid coated with carbon film and the water evaporated under atmospheric pressure at room temperature for 2 days.

3. Results and discussion

3.1. Synthesis of PMOMA backbone

Since acrylic acid cannot be polymerized by ATRP, we should choose a poly(acrylate) backbone which can be formed via ATRP and selectively hydrolyzed to PAA backbone compared with PMMA branches. *tert*-Butyl acrylate is maybe a good choice due to its successful polymerization via ATRP and acidic hydrolysis conditions with CF_3COOH, but has no effect on PMMA [10,17]. Unfortunately, it was difficult to introduce ATRP initiation groups to poly(*tert*-butyl acrylate) backbone by reacting with LDA and α-bromoisobutyryl bromide, which might be attributed to steric effect. Thus, methoxymethyl acrylate was selected as the monomer to synthesize the backbone for its mild acidic hydrolysis conditions without steric effect. PMOMAs with narrow molecular weight distributions ($M_w/M_n < 1.25$) were obtained via ATRP at 50 °C as shown in Table 1. The yields are relatively high (≥60%) and the molecular weights could be easily tuned by varying the feed ratios. For PMOMAs **1a** and **1b**, every chain has about 29.6 and 55.5 MOMA repeating units, respectively.

The GPC chromatograph (RI) of PMOMA **1a** is shown in Fig. 1. The unimodal and symmetrical GPC curve with narrow molecular weight distribution ($M_w/M_n = 1.14$) confirmed the successful ATRP [15]. We also used an UV detector ($\lambda =$ 260 nm) to check the possible side reactions, which can form β-ketoester by backbiting of the ester enolate chain end [22]. The result demonstrated the absence of side reactions.

Table 1
Polymerization of MOMA by ATRP[a]

PMOMA	[MOMA]:[2-MBP]	Time (h)	M_n[b] (g/mol)	M_w/M_n[b]	Yield (%)	Br[c] (%)
1a	26:1	2.5	3600	1.14	78	2.21
1b	53:1	8.5	6600	1.10	60	0.62
1c	78:1	12	11,000	1.21	69	–

[a] Feed ratio: [CuBr]:[PMDETA]:[2-MBP] = 1:1:1, polymerization temperature: 50 °C.
[b] Measured by GPC.
[c] Obtained from the titration with $Hg(NO_3)_2$.

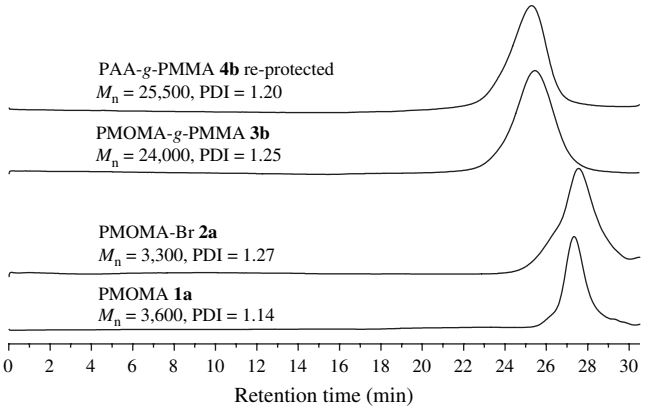

Fig. 1. GPC traces of PMOMA **1a**, macroinitiator **2a**, PMOMA-*g*-PMMA **3b**, and reprotected PAA-*g*-PMMA **4b** in THF.

After polymerization, the resonance peaks of the double bond protons in ^1H NMR spectrum disappeared and the signals of poly(acrylate) backbone appeared at $\delta = 1.37-5.16$ ppm. ATRP mechanism of the polymerization can be confirmed by the resonance peak of CH_3 protons at 1.09 ppm of the initiation group at one end and the resonance peak of C*H*Br proton at 4.25 ppm at the other end.

3.2. Synthesis of PMOMA-Br macroinitiator

In previous literatures [10,17], graft copolymers having a hydrophobic backbone and hydrophilic side chains could be easily prepared by ATRP and grafting-from techniques since the ester groups of the backbone could be easily converted to the halogen-containing ATRP initiation groups. To retain the ester groups on the backbone so that they can be hydrolyzed to the hydrophilic carboxylic groups, a novel method was developed by our group to connect ATRP initiation groups to the α-carbon of the ester groups using LDA and α-bromoisobutyryl bromide [19,20]. Ester groups of PMOMA backbone and C–Br groups of ATRP initiation groups were supposed to experience no affection, as evidenced from the previous literature [23] (Scheme 3).

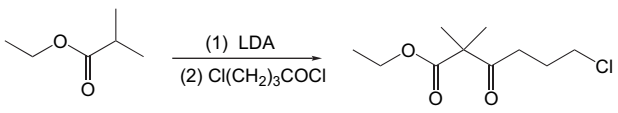

Scheme 3. Model reaction for the introduction of ATRP initiation group.

Table 2
Characterization of macroinitiators **2a** and **2b**

Macroinitiator	M_n (g/mol)	M_w/M_n[c]	Br[d] (%)	Grafted ATRP initiation group density
2a[a]	3300	1.27	8.83	1/7
2b[b]	6200	1.23	11.25	1/5

[a] Compound **2a** was prepared from PMOMA **1a**.
[b] Compound **2b** was prepared from PMOMA **1b**.
[c] Measured by GPC.
[d] Obtained from the titration with $Hg(NO_3)_2$.

By this approach, PMOMA **1** was successfully transformed into the macroinitiator and ATRP initiation groups were connected to poly(acrylate) backbone through stable C–C bonds instead of ester connections.

The successful introduction of ATRP initiation groups into PMOMA backbone was confirmed by the increase of bromine content of macroinitiators (2.21–8.83% for **2a** and 0.62–11.25% for **2b**, listed in Table 2) and NMR.

^{1}H NMR spectrum of PMOMA-Br **2** is shown in Fig. 2. All the corresponding signals of the protons of PMOMA backbone are observed. It was found that the integration area of the peak at 1.97 ppm obviously increased due to the newly introduced six protons of $COC(CH_3)_2Br$ of ATRP initiation groups. Also, no signal of alkene was found in the region between 4.5 and 7.0 ppm, which concludes to the fact that the possible elimination reaction of CHBr end group did not occur during the chemical modification with LDA and α-bromoisobutyryl bromide.

^{13}C NMR spectrum of PMOMA-Br **2** is shown in Fig. 3. The appearance of a new peak at 207.4 ppm (the keto carbon

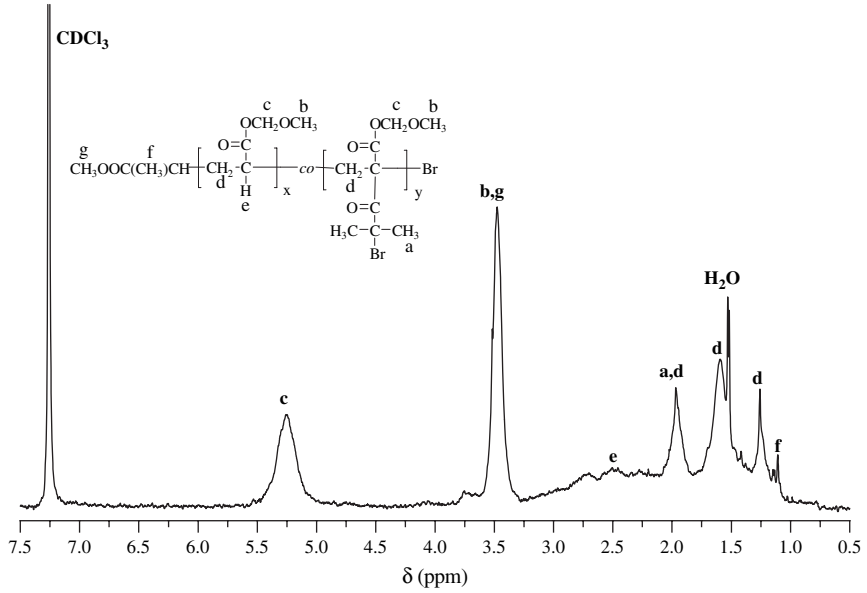

Fig. 2. ^{1}H NMR spectrum of PMOMA-Br **2** macroinitiator.

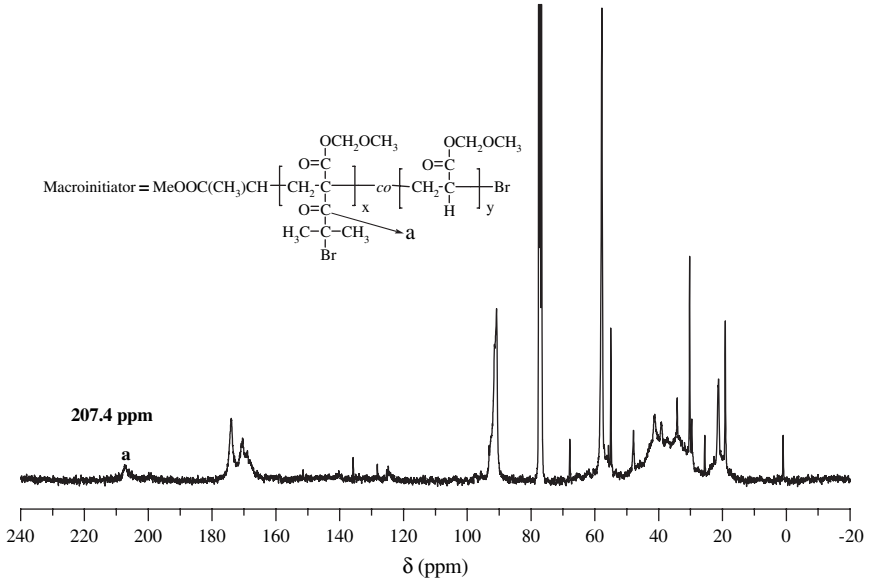

Fig. 3. ^{13}C NMR spectrum of PMOMA-Br **2** macroinitiator.

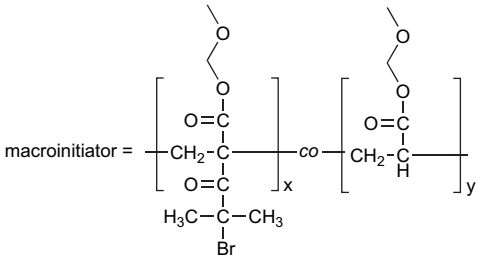

Scheme 4. Chemical structure of macroinitiator **2**.

of $-CO(CH_3)_2Br$) also indicated the successful synthesis of macroinitiator **2**.

Since the peak of the protons of $COC(CH_3)_2Br$ overlapped with that of PMOMA backbone, it was difficult to calculate the density of the grafted ATRP initiation group from ^1H NMR. The structure of macroinitiator is as indicated in Scheme 4. From the results of Br% of macroinitiator **2**, the approximate grafted ATRP initiation group density can be calculated. The molecular weight of *x* part (incorporated with ATRP initiation group) and *y* part is 265 and 116, respectively. The bromine content of **2a** was 8.83%, the ratio of *x*/*y* of **2a** was calculated to be 1/6 according to Eq. (1)

$$80x/(265x + 116y) = 0.0883 \quad (1)$$

Also, the ratio of *x*/*y* of **2b** was calculated to be 1/4. So the approximate grafted ATRP initiation group densities of **2a** and **2b** are 1/7 for **2a** and 1/5 for **2b**, which meant ATRP initiation groups were introduced to one seventh or one fifth of the repeating units of PMOMA backbone. Because every chain of PMOMAs **1a** and **1b** has 29.6 and 55.5 MOMA repeating units, PMOMA-Br **2a** and **2b** has about 4.2 and 11.1 ATRP initiation groups, respectively.

As shown in Fig. 1, only a unimodal peak was found in the GPC chromatograph of PMOMA-Br **2a** after the reaction with LDA and α-bromoisobutyryl bromide. The molecular weight distribution is still narrow ($M_w/M_n = 1.27$) so that it can be concluded that the architecture of polymer chain was not destroyed. The M_n of PMOMA-Br **2a** macroinitiator ($M_n =$ 3300) was a little smaller than that of PMOMA **1a** ($M_n =$ 3600) due to the newly branched ATRP initiation groups, which was similar with our previous report [24].

3.3. Graft copolymerization of MMA

ATRP of MMA was initiated by macroinitiator **2** at 50 °C as listed in Table 3. All graft copolymers' molecular weights were much higher than that of the macroinitiator, which concludes that the polymerization of MMA was performed. The molecular weights of graft copolymers increased with the extending of polymerization time, which is the characteristic of ATRP. All graft copolymers showed unimodal and symmetrical GPC curves (Fig. 1) with narrow molecular weight distributions ($M_w/M_n \leq 1.30$), which are characteristic of ATRP [15] and also indicated that intermolecular coupling reactions could be neglected [17]. It was found that a high feed ratio of monomer to initiator and a low conversion (<10%) were necessary to suppress the intermolecular coupling reactions, which is similar with previous studies [10,17,25–29].

Table 3
Synthesis of PMOMA-*g*-PMMA graft copolymers

Copolymer	Time (min)	Conv.[c] (%)	M_n[d] (g/mol)	M_w/M_n[d]	N_{MOMA}/N_{MMA}[e]
3a[a]	5	–	17,000	1.19	1/6
3b[a]	10	2.6	24,000	1.25	1/9
3c[a]	15	4.1	32,000	1.27	1/21
3d[a]	20	4.3	37,000	1.25	1/45
3e[a]	30	6.9	44,000	1.28	1/59
3f[b]	15	1.3	26,000	1.21	1/7
3g[b]	20	3.0	33,000	1.29	1/11
3h[b]	30	9.9	53,000	1.30	1/18

[a] Initiated by **2a**, [MMA]:[Br group]:[CuBr]:[dHbpy] = 500:1:1:2.
[b] Initiated by **2b**, [MMA]:[Br group]:[CuBr]:[dHbpy] = 500:1:1:2.
[c] Determined by GC.
[d] Measured by GPC.
[e] Obtained by ^1H NMR.

The signals of the corresponding protons of PMOMA backbone and PMMA side chains were found in ^1H NMR spectrum as shown in Fig. 4A. The ratio of total number of MOMA unit to MMA unit (N_{MOMA}/N_{MMA}) could be calculated from ^1H NMR according to Eq. (2) as listed in Table 3 (S_c is the integration area of two protons of OCH_2 of PMOMA backbone at 5.21 ppm, S_{a+b} is the total integration area of three protons of CH_2OCH_3 of PMOMA backbone at 3.45 ppm and three protons of $COOCH_3$ of PMMA side chains at 3.57 ppm)

$$N_{MOMA}/N_{MMA} = [S_c/2]/[(S_{a+b} - 1.5\ S_c)/3] \quad (2)$$

3.4. Hydrolysis of PMOMA-*g*-PMMA

Hydrolysis of PMOMA-*g*-PMMA **3** was carried out under mild acid conditions. PAA-*g*-PMMA **4** amphiphilic graft copolymer is soluble in THF, 1,4-dioxane and *N*,*N*-dimethylformamide. For GPC analysis, PAA backbone was reprotected by CH_2N_2 to be transformed into poly(methyl acrylate) backbone. A unimodal GPC peak, whose shape and position was almost identical with that of PMOMA-*g*-PMMA **3** prior to hydrolysis, was observed in Fig. 1. Therefore, the hydrolysis process did not destroy the structure of graft copolymer.

The structure of the hydrolyzed product was characterized by ^1H NMR and FT-IR. The disappearance of the signals of the methoxymethyl protons at 3.45 and 5.21 ppm in ^1H NMR spectrum (Fig. 4B) assured the complete hydrolysis of PMOMA backbone. The appearance of a broad peak of –COOH at 3457 cm^{-1} in FT-IR spectrum (Fig. 5) indicated the formation of PAA backbone.

The ester groups of PMMA branches were not hydrolyzed since the resonance peak of $COOCH_3$ protons was found to remain at 3.59 ppm in ^1H NMR spectrum and the peak area was not altered with an increase of the hydrolysis time. Therefore, it can be concluded that PMOMA-*g*-PMMA was selectively hydrolyzed to PAA-*g*-PBMA.

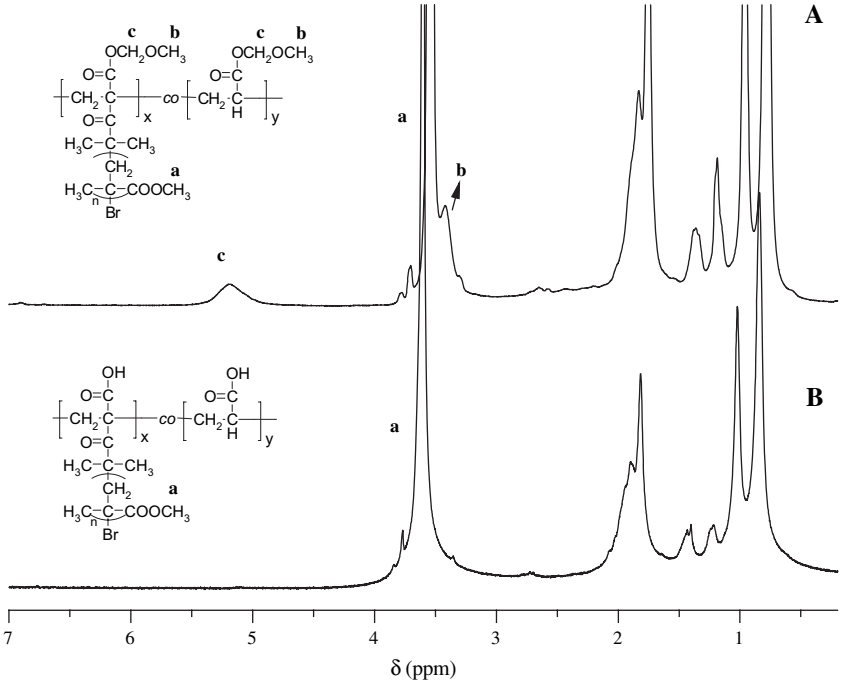

Fig. 4. ^{1}H NMR spectra of PMOMA-*g*-PMMA (A) and PAA-*g*-PMMA (B).

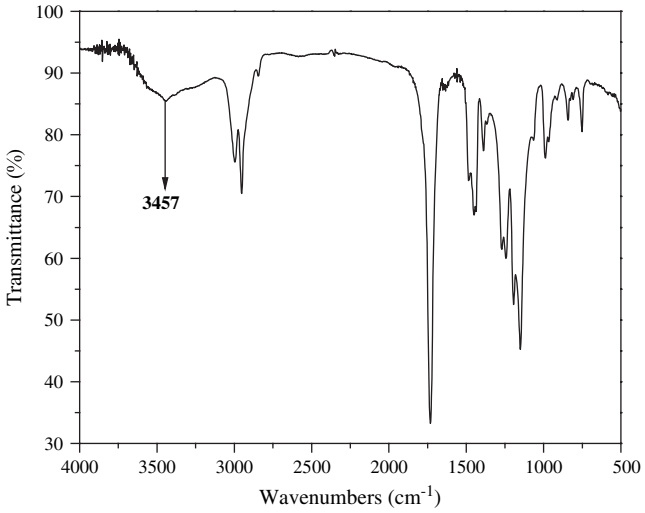

Fig. 5. FT-IR spectrum of PAA-*g*-PMMA **4**.

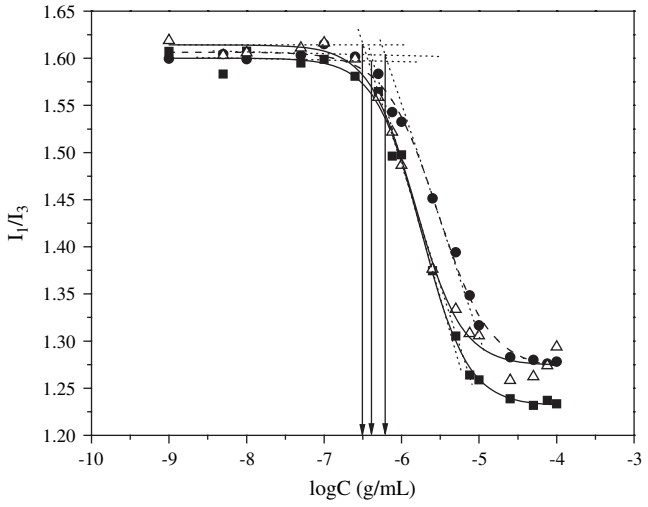

Fig. 6. Dependence of fluorescence intensity ratios of pyrene emission bands on the concentrations of PAA-*g*-PMMA **4** (●: **4b**, □: **4d**, △: **4e**).

3.5. Measurement of critical micelle concentration

The cmc values of PAA-*g*-PMMA **4** amphiphilic graft copolymers in the aqueous solution were examined by fluorescence technique using pyrene as probe [30,31]. Fluorescence spectrum of pyrene is sensitively affected by the environment and the polarity of its surrounding [30,31]. In the presence of micelles, pyrene is solubilized within the interior of the hydrophobic part. As a result, the values of I_1/I_3 of the emission spectrum changed sharply. The ratios of the intensity (I_1/I_3) against the logarithm of polymer concentrations were plotted to determine cmc as the onset of micellization (Fig. 6).

Table 4
Critical micelle concentrations of amphiphilic graft copolymers

Copolymer	N_{AA}/N_{MMA}	cmc (g/mL)
4b	1/9	5.62×10^{-7}
4d	1/45	4.68×10^{-7}
4e	1/59	3.39×10^{-7}

As shown in Table 4, the cmc values of PAA-*g*-PMMA amphiphilic graft copolymers with different molecular weights were all approximately 10^{-7} g/mL, which were very low compared with those of traditional surfactants [32] and indicated the formation of the stable micelles with the low rates of

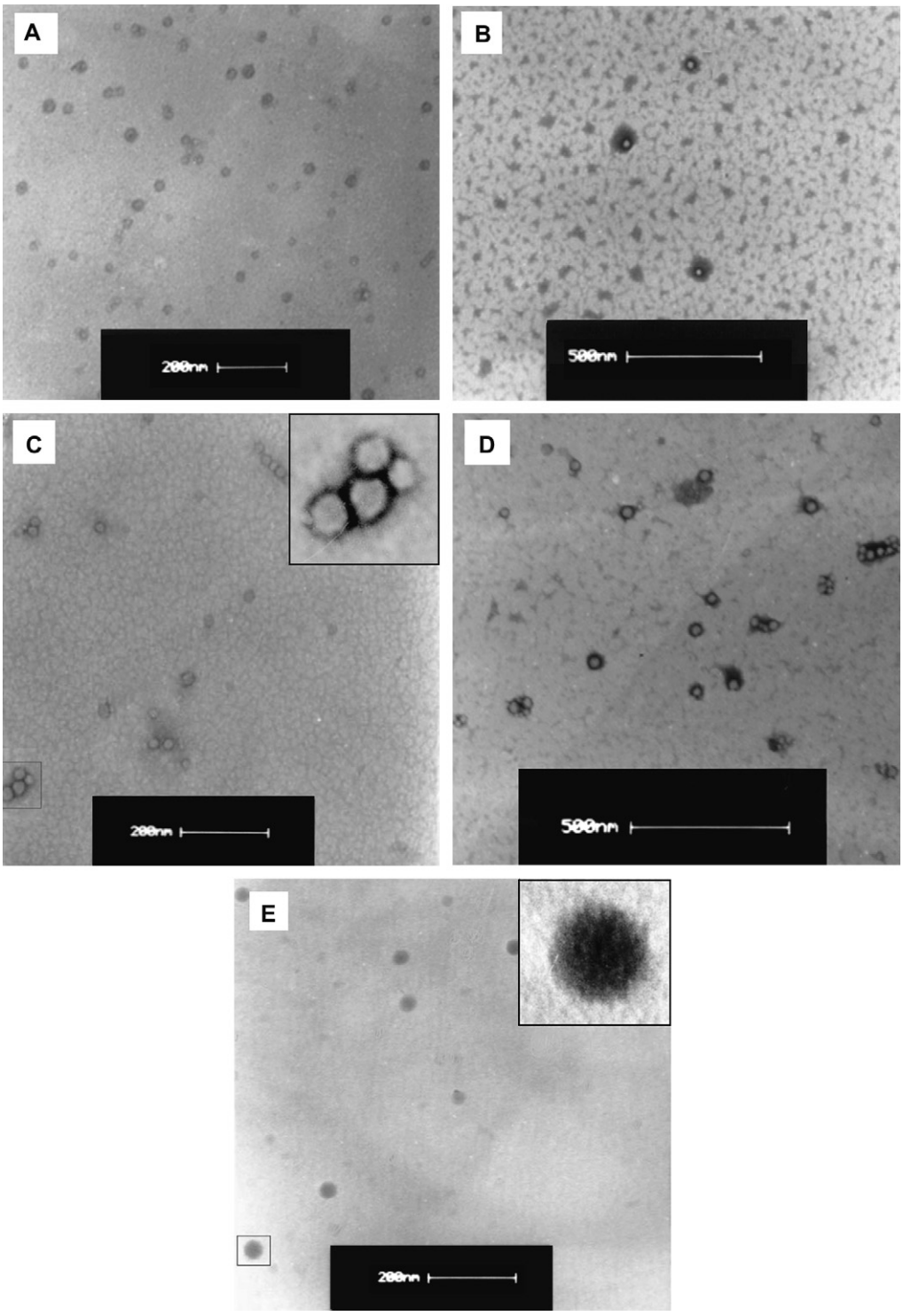

Fig. 7. TEM images of micelles of PAA-*g*-PMMA **4d** (A), PAA-*g*-PMMA **4e** (B) and PAA-*g*-PMMA **4f** (C) in water (freshly prepared); PAA-*g*-PMMA **4d** (D) in water (two weeks after preparation); PAA-*g*-PMMA **4f** (E) in 1 wt% NaCl solution. (B, C, and D were negatively stained by phosphotungstic acid.)

dissociation [33]. These low values were attributed to the branched structure of the graft copolymers and a high percentage of the hydrophobic side chains. Also, the cmc values decreased slightly with the large increase of the contents of PMMA side chains (the ratio of N_{AA}/N_{MMA} changed from 1/9 to 1/59). Thus, we can conclude that the cmc values of PAA-*g*-PMMA amphiphilic graft copolymers were not sensitive to the ratios of N_{AA}/N_{MMA}, which was similar with the previous literature [34].

3.6. Micellar morphologies

Samples for TEM analysis were prepared by the evaporation of the solvent at atmospheric pressure and room

temperature [35,36]. TEM images of the micelles of PAA-*g*-PMMA **4** amphiphilic graft copolymers in the fresh aqueous solution are shown in Fig. 7A–C. It was found that the micelles formed by PAA-*g*-PMMA amphiphilic graft copolymers with different molecular weights were all vesicles (ca. 30–50 nm).

A two-step self-assembly process was suggested for the formation of vesicles [37]. At first, the amphiphilic copolymer forms a bilayer; next, the bilayer closes to form a vesicle. It is well known that the degree of stretching decreases as the morphology changes from the spheres to the cylinders and to the vesicles, because the additional degree of freedom along the axis or the plane allows more chains in the cylinders or in the bilayers to be incorporated into the structure without significant changes in their conformation [2,3], which was same in our studies. PMMA is a kind of polymer with weak hydrophobicity and has interaction with water through the ester groups [38]. When PAA-*g*-PMMA was added to water from THF, the changing of the conformation of PMMA side chains was not significant and the degree of stretching of PMMA side chains was kept low, which were helpful for the formation of vesicles. The obtained vesicles were stable and retained the original morphology for at least two weeks (Fig. 7D).

The micelles formed by PAA-*g*-PMMA amphiphilic graft copolymers changed from the vesicles to the spheres as the electrolyte, NaCl, was added to water (Fig. 7E). This can be explained that the addition of NaCl destroyed the interactions between PMMA, PAA and water, so the polarity of the solution increased and the swelling extent of PMMA side chains decreased. As a result, the degree of stretching of PMMA side chains in water increased and the spheres were preferred to be formed.

4. Conclusion

A series of well-defined amphiphilic graft copolymer consisting of hydrophilic PAA backbone and hydrophobic PMMA side chains were synthesized by the combination of ATRP and grafting-from techniques. These amphiphilic graft copolymers have cmc values as low as 10^{-7} g/mL. The micelles formed by PAA-*g*-PMMA with different molecular weights were vesicles, which were related with the interactions between PMMA side chains and water. The addition of NaCl to water made the micelles turn into spheres due to the destruction of the interactions between PMMA side chains and water. These findings enriched the self-assembly studies of amphiphilic copolymers from both theoretical and experimental points.

Acknowledgement

The authors thank the financial support from National Natural Science Foundation of China (Grant no. 20404017).

References

[1] Halperin A, Tirrell M, Lodge TP. Adv Polym Sci 1992;100:31.
[2] Zhang L, Eisenberg A. J Am Chem Soc 1996;118:3168.
[3] Zhang L, Yu K, Eisenberg A. Science 1996;272:1777.
[4] Zhang L, Eisenberg A. Macromolecules 1996;29:8805.
[5] Forder C, Patrickios CC, Armes SP, Billingham NC. Macromolecules 1996;29:8160.
[6] Thurmond KB, Kowalewski T, Wooley KL. J Am Chem Soc 1997;119:6656.
[7] Maskos M, Harris JR. Macromol Rapid Commun 2001;22:271.
[8] Ma Y, Cao T, Webber SE. Macromolecules 1998;31:1773.
[9] Kikuchi A, Nose T. Macromolecules 1996;29:6770.
[10] Zhang M, Breiner T, Mori H, Müller AHE. Polymer 2003;44:1449.
[11] Percec V, Aszgarzadeh F. J Polym Sci Polym Chem 2001;39:1120.
[12] Xu X, Huang J. J Polym Sci Polym Chem 2006;44:467.
[13] Shi Y, Fu Z, Yang W. J Polym Sci Polym Chem 2006;44:2069.
[14] Li Z, Li P, Huang J. J Polym Sci Polym Chem 2006;44:4361.
[15] Wang J, Matyjaszewski K. J Am Chem Soc 1995;117:5614.
[16] Matyjaszewski K, Xia J. Chem Rev 2001;101:2921.
[17] Cheng G, Boker A, Zhang M, Krausch G, Müller AHE. Macromolecules 2001;34:6883.
[18] Zhang H, Ruckenstein E. Macromolecules 2000;33:814.
[19] Peng D, Zhang XH, Huang XY. Polymer 2006;47:6072.
[20] Peng D, Lu GL, Zhang S, Zhang XH, Huang XY. J Polym Sci Polym Chem 2006;44:6857.
[21] Leduc MR, Hawker CI, Dao J, Frechet JMJ. J Am Chem Soc 1996;118:11111.
[22] Janata M, Lochmann L, Müller AHE. Makromol Chem 1990;191:2253.
[23] Kocienski PJ, Narquizian R, Raubo P, Smith C, Boyle FT. Synlett 1998;869.
[24] Peng D, Zhang XH, Huang XY. Macromolecules 2006;39:4945.
[25] Matyjaszewski K, Qin S, Boyce JR, Shirvanyants D, Sheiko SS. Macromolecules 2003;36:1843.
[26] Beers KL, Gaynor SG, Matyjaszewski K. Macromolecules 1998;31:9413.
[27] Liu S, Ayusman S. Macromolecules 2000;33:5106.
[28] Borner HG, Beers K, Matyjaszewski K. Macromolecules 2001;34:4275.
[29] Shen Z, Chen Y, Barriau E, Frey H. Macromol Chem Phys 2006;207:57.
[30] Kalyanasundaram K, Thomas J. J Am Chem Soc 1977;99:2039.
[31] Wilhelm M, Zhao C, Wang Y, Xu R, Winnik M, Mura J, et al. Macromolecules 1991;24:1033.
[32] Lavasanifar A, Samuel J, Kwon G. Colloids Surf B Biointerfaces 2001;22:115.
[33] Allen C, Maysinger D, Eisenberg A. Colloids Surf B Biointerfaces 1999;16:3.
[34] Xu P, Tang H, Li S, Ren J, Kirk EV, Murdoch WJ, et al. Biomacromolecules 2004;5:1736.
[35] Shen H, Zhang L, Eisenberg A. J Am Chem Soc 1999;121:2728.
[36] Luo L, Eisenberg A. Langmuir 2001;17:6804.
[37] Antonietti M, Förster S. Adv Mater 2003;15:1323.
[38] Sutander P, Ahn DJ, Franses EI. Macromolecules 1994;27:7316.